

Estimates of station misorientation from surface-wave arrival-angle data

Erik W.F. Larson, Göran Ekström, and Jeroen Tromp

Department of Earth and Planetary Sciences, Harvard University, Cambridge, MA 02138. E-mail: ErikLarson@iname.com

Summary:

In order to refine global seismic structure of the upper mantle, we have made many measurements of arrival angles of surface waves. As a by-product of this investigation we have determined that the horizontal components of some seismometers are misaligned, i.e. the true azimuths are not correctly reported to the data centers. We have carefully examined our data to isolate other possible effects, and here we present our estimates of the misalignment of seismometers, in order that they can be field-checked.

Introduction

The path of a seismic wave is dependent on the velocities of the material through which it travels. Since the arrival angle is a snapshot of the ray path, measurements of arrival angle provide information about the velocities along the path. A linear relationship between arrival angle and gradients in phase velocity has been determined for fundamental-mode surface waves (Woodhouse & Wong, 1989). We developed a new automated technique to measure arrival angle, and have collected a large data set of observations. We then try to interpret the observations in terms of phase velocity structure. However, we found, as Laske (1994) found for a smaller set of stations, that the data clearly show that some seismometers are misaligned.

Measurement Technique

We measure arrival angles of intermediate period (50-125s) first-orbit surface waves using an automated technique. The first step in this method is obtaining a reliable estimate of the phase dispersion of the surface wave, which we get through the automated method of Ekström, et. al (1997). We use these phase dispersion measurements from the vertical-component Rayleigh wave to create a synthetic seismogram with correct phase. We compare this synthetic with the longitudinal component of the data seismogram. We then measure the best-fit smooth amplitude spectrum. We combine the phase and the new amplitude measurements to make another synthetic seismogram of the longitudinally polarized Rayleigh wave, which we subtract from the data. Now we create a synthetic seismogram of the Love wave using the phase measurements, which we use as a phase matched filter. We divide the two horizontal component data seismograms by the synthetic, which would create a time-domain delta function if we had exactly matched the phase and the Love wave were the only signal. We band pass each of these with several

narrow frequency windows. Then, for each frequency window, we measure the relative amplitude of the two components in a narrow time window around the center of the delta function. This relative amplitude is the tangent of the apparent arrival angle in the frequency band. Also, as error estimates, we measure the consistency of the measurement across this time window and the amount of noise outside the window. We then follow the same procedure to measure Rayleigh waves: subtract the Love wave, isolate the Rayleigh wave, and measure the relative amplitude of two horizontal components.

Data

Our data set for making measurements covers the period 1989-1997. The earthquakes included are those with $M_w > 5.5$ in the Harvard CMT catalog, and we use data recorded on the GSN, leading to a database of over 125,000 three-component digital seismograms. We use the most current nominal station orientations reported to us for each earthquake. We select only shallow earthquakes and use paths with epicentral distances in the range 30 to 150 degrees. At various stages, we assess the error estimate and discard poor measurements. In the end, we have measurements of Love wave arrival angles from over 18,000 earthquake-station pairs and of Rayleigh wave arrival angles from over 15,000 pairs.

Analysis

As a first step in analyzing the data, for each station we look at all the measurements. Although for most stations there is no consistent deviation from great circle arrival angle, we see that for some stations, there is a clear bias of arrival angle, both for Rayleigh and Love waves (Fig 1). We investigate possible variations of arrival angle which vary with back azimuth, but no pattern is apparent for any station. We also look for variations as a function of time, and there are hints of changes at some stations, but we do not have sufficient data to be certain. Therefore, the raw data show that some seismometers appear to be rotated.

However, it is possible that there can be a trade-off station "rotation" and effects of refraction due to velocity structure. Therefore, taking a simple average or median of all the measurements at a station may not give the correct effect of the station. We attempt to determine the misorientation effect of each station and the refraction effects simultaneously. We use measurements of Rayleigh waves and Love waves at five periods: 50s, 60s, 75s, 100s, and 125s. In our model, we have a phase velocity map for each wave type

and period and *only one* station term for each station. The maps are expanded in spherical harmonics to degree 20. We use a least-squares inversion of the whole data set, with various levels of damping on the first derivative of the phase velocity maps. Also, we have used the same model and included phase dispersion data, which constrain the maps but not the station terms, and then we do not need to add damping. All inversions produce very similar station terms (Fig 2), indicating that we have isolated the velocity structure from the station terms.

There are other possible sources of error, and we performed several tests to determine errors in the measurement technique. We created normal-mode synthetic seismograms using PREM and followed the measurement technique outlined above. We obtained individual measurement errors of one to two degrees, primarily due to the influence of overtones. Also, we determined empirical estimates using pairwise-similar paths, comparing the measurements made at one station from several earthquakes close to each other. These 1σ errors are around one to two degrees for our best quality paths, and up to four degrees for lower quality paths.

Conclusion

The results we present are our best estimates of the misreported orientation of seismometers (Table 1). It is possible that some apparent seismometer misorientations are a result of effects not included in our study, such as large near-station effects. The errors we show are estimates of what we believe we can resolve. They are based on the amount and quality of measurements from each station.

References

Ekström, Göran, Jeroen Tromp, and Erik W. F. Larson, 1997. Measurements and global models of surface wave propagation, *J. geophys. Res.*, **102**(B4), 8137-8157.

Laske G., G. Masters, and W. Zürn, 1994. Frequency-dependent polarization measurements of long-period surface waves and their implications for global phase-velocity maps, *Phys. Earth Plan. Int.*, **84**, 111-137.

Woodhouse, J. H. and Y.K. Wong, 1986. Amplitude, phase and path anomalies of mantle waves, *Geophys. J. R. astr. Soc.*, **87**, 753-773.

Table 1: Seismometer rotation estimates. First column is station name, second column is rotation estimate, third column is estimated errors. Asterisks (*) mark stations for which rotation estimate is greater than twice the estimated error.

AAK	5.9	3.0	DPC	1.7	3.6	KONO	-0.9	1.7	RAR	0.1	2.8
ADK	-0.0	3.9	ENH	-2.0	2.1	LPAZ	0.8	3.7	RPN	0.9	3.3
AFI	2.0	3.1	ERM	-0.3	3.2	LSA	-2.2	2.7	SBC	-1.2	3.1
ALE	-1.7	2.1	ESK	1.6	2.1	LSZ	-3.1	4.4	SDV	-0.9	5.0
ANMO	2.2	1.4	FFC	2.2	2.5	LVZ	0.8	2.2	SNZO	6.5	2.0 *
ANTO	-0.3	3.0	GDH	-2.3	4.9	LZH	2.9	1.2 *	SPA	-2.9	4.5
ARU	-0.1	3.6	GRFO	5.2	2.2 *	MA2	-3.0	4.9	SSE	-5.1	3.1
BAR	-4.4	4.7	GSC	-1.0	2.6	MAJO	-3.4	1.6 *	SUR	-1.4	2.2
BGCA	11.1	5.2 *	GUMO	-2.8	2.1	MDJ	-1.0	1.7	TATO	-10.3	3.2 *
BJI	1.3	2.8	HIA	-0.6	1.3	MSVF	-10.2	4.8 *	TAU	-2.7	2.6
BJT	-0.1	2.6	HKT	2.3	4.7	NNA	0.7	3.2	TLY	3.6	2.0
BOSA	-1.2	2.7	HNR	-6.0	3.0 *	NRIL	0.3	3.3	TOL	1.3	4.2
BRVK	0.1	4.4	HRV	0.3	1.5	NWAO	4.0	1.2 *	TUC	-0.5	1.9
CAN-G	0.1	3.5	INU-G	-0.8	4.5	OBN	-0.1	2.2	ULN	-3.9	3.6
CCM	-0.1	2.2	ISA	1.9	2.3	PAB	0.4	2.3	WMQ	1.0	1.5
CHTO	1.8	1.6	KBS	-0.7	3.6	PAS	-1.0	1.5	WRAB	0.5	2.9
CMB	-3.1	1.7	KEV	-4.2	1.6 *	PET	4.9	3.4	WUS-G	-1.7	4.8
COL	-0.8	2.1	KIEV	0.6	3.2	PFO	0.2	2.1	XAN	-1.2	4.2
COR	-0.8	1.6	KIP	-0.8	1.4	PLCA	1.3	2.8	YAK	-2.8	3.8
CTAO	1.1	1.4	KIV	6.6	4.4	PMG	0.3	3.0	YSS	0.6	3.1
DBIC	14.2	6.4 *	KMI	0.1	1.4	QIZ	-0.6	2.7			

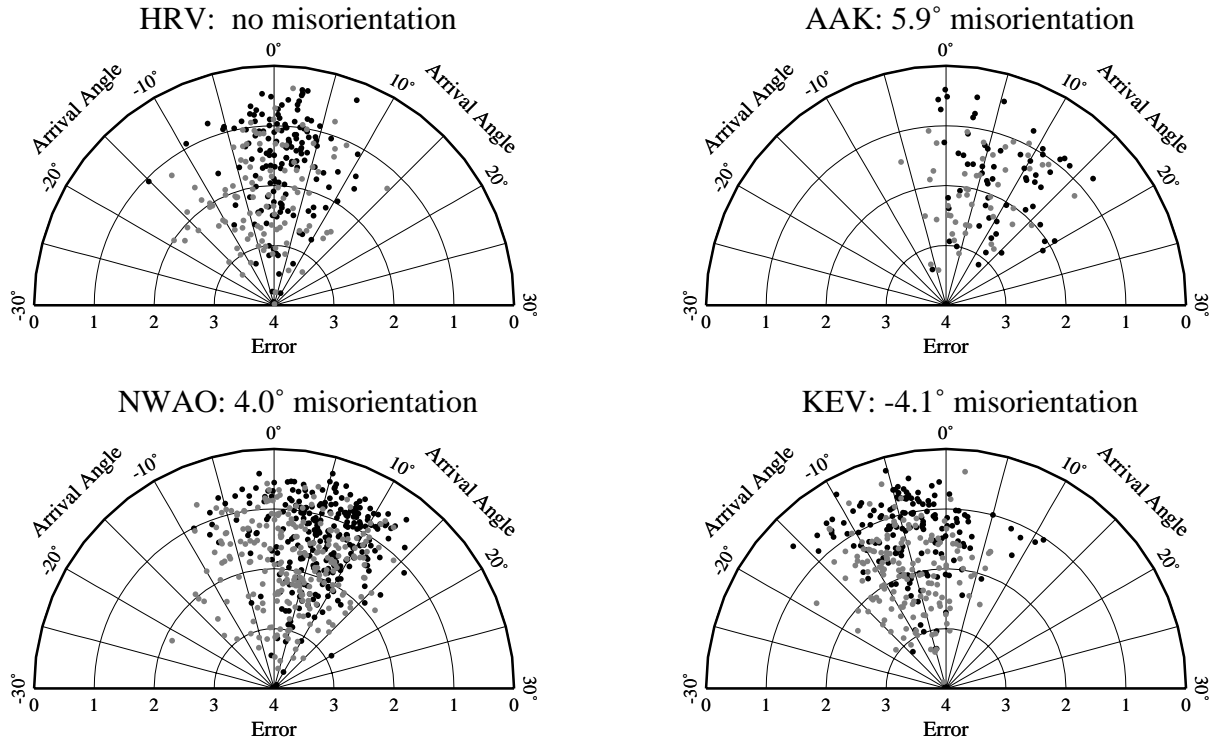


Figure 1: Examples of observations of surface wave arrival angle at four stations. Light symbols are arrival angles of Rayleigh waves at 100s period, and dark symbols are for Love waves at 75s period. Note that the quality (inverse of error) increases from the center of each diagram.

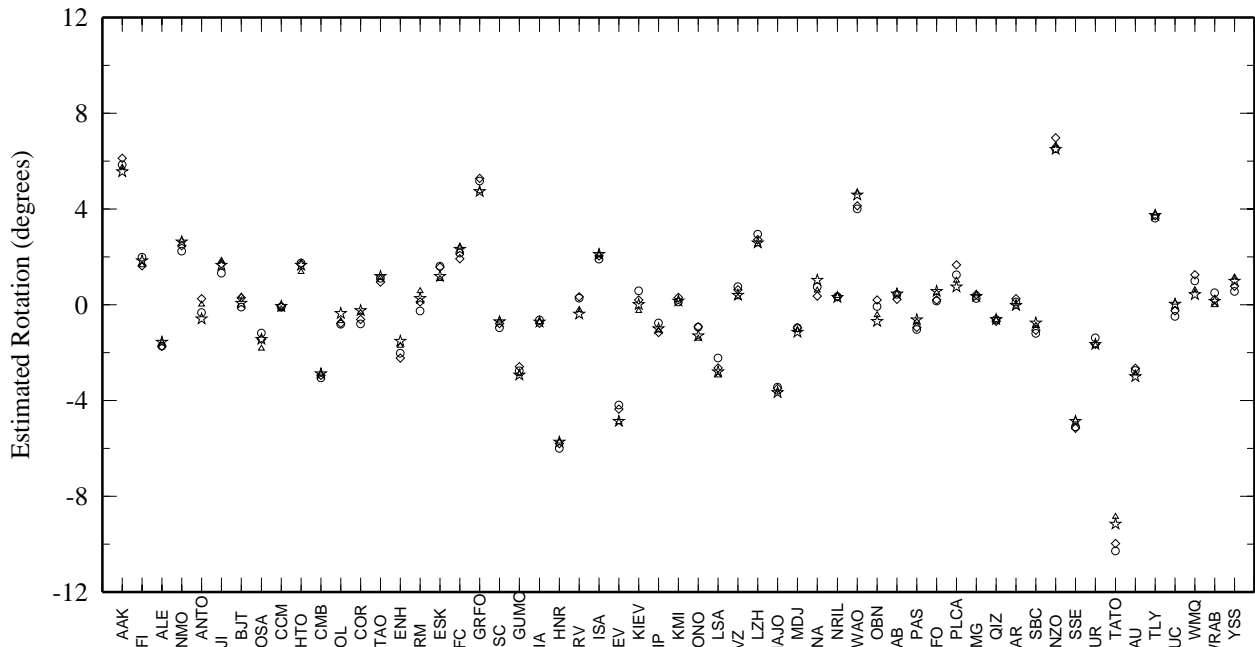


Figure 2: Seismometer rotation obtained when phase velocity structure is varied: expanding the phase velocity degree 16 or degree 20, and including just arrival angle data or both arrival angle and phase data (four symbols for each station).